Phase-enhanced defect sensitivity for EUV mask inspection

Yow-Gwo Wang[a, b], Ryan Miyakawa[a], Weilun Chao[a], Kenneth Goldberg[a],
Andy Neureuther[a, b], and Patrick Naulleau[a]
[a]Center for X-ray Optics, Lawrence Berkeley National Laboratory, Berkeley, CA, 94720
[b]Department of Electrical Engineering and Computer Sciences, University of California, Berkeley, CA, 94720

ABSTRACT

In this paper, we present a complete study on mask blank and patterned mask inspection utilizing the Zernike phase contrast method. The Zernike phase contrast method provides in-focus inspection ability to study phase defects with enhanced defect sensitivity. However, the 90 degree phase shift in the pupil will significantly reduce the amplitude defect signal at focus. In order to detect both types of defects with a single scan, an optimized phase shift instead of 90 degree on the pupil plane is proposed to achieve an acceptable trade-off on their signal strengths. We can get a 70% of its maximum signal strength at focus for both amplitude and phase defects with a 47 degree phase shift. For SNR, the trade-off between speckle noise and signal strength has to be considered. The SNR of phase and amplitude defects at focus can both reach 11 with 13 degree phase shift and 50% apodization. Moreover, the simulation results on patterned mask inspection of partially hidden phase defects with die-to-database inspection approach on the blank inspection tool show that the improvement of the Zernike phase method is more limited. A 40% enhancement of peak signal strength can be achieved with the Zernike phase contrast method when the defect is centered in the space, while the enhancement drops to less than 10% when it is beneath the line.

Keywords: EUV Mask Inspection, Native Defect, Zernike Phase Contrast Microscope.

1. INTRODUCTION

A defect free EUV mask blank is needed for EUV lithography to be ready for high-volume manufacturing. To achieve this, actinic inspection will likely be required [1]. However, the conventional EUV mask inspection tool has to do multiple scans at different defocus levels to gather both amplitude and phase defect information; thus impacting the throughput. The Zernike phase contrast method which can observe phase defects at focus is a promising technique to improve inspection efficiency.

In our previous study [2], Zernike phase contrast microscopy showed in-focus inspection ability to identify phase defects on EUV mask blanks. By adding a 90 degree phase shifts to the pupil plane, the phase defect information is transformed to intensity, yielding enhanced defect image contrast at focus. Moreover, this signal can be even further strengthened by partial attenuation of the DC term in the pupil. The pupil plane apodization also serves to reduce the speckle noise by cutting of its low frequency contribution to the aerial image, so we can achieve a better signal-to-noise ratio (SNR).

In this paper, we extend our inspection target to both amplitude and phase defects on the mask blank and to patterned mask inspection. An optimized phase shift in the pupil plane can produce acceptable trade-off between phase and amplitude defect signal strength compared to conventional imaging methods. We also apply the phase contrast method to patterned mask inspection and discuss the possibility of improving the SNR at focus for critical defects.

2. BACKGROUND

2.1 Optical principle for phase contrast and apodization

Zernike phase contrast microscopy was proposed at 1953 and has been widely used since then [3]. From the EUV mask inspection perspective, the phase shift and apodization in the system can rotate and attenuate the DC term to achieve better contrast for phase defects. Thus we can observe phase defects at focus with high sensitivity. In addition, the speckle noise can be reduced by apodization in the pupil plane when the apodization area surrounds and includes the illumination. This is because the phase roughness of the mask is dominated by low frequencies that diffract at low angles.

Photomask Technology 2014, edited by Paul W. Ackmann, Naoya Hayashi, Proc. of SPIE
Vol. 9235, 92350L · © 2014 SPIE · CCC code: 0277-786X/14/$18 · doi: 10.1117/12.2069291

A schematic diagram explaining the advantages of the phase contrast method to EUV mask inspection is shown in Figure 1.

The idea of reduced speckle noise can be explained by the roughness power spectral density (PSD). The roughness PSD shown in Figure 2 is measured by scatterometry from a EUV mask [4]. The black dashed line indicates the maximum spatial frequency of the optical system and the shaded area represents the apodization region. Simulation shows that a 75% reduction in speckle noise is achieved with 25% apodization in the pupil plane.

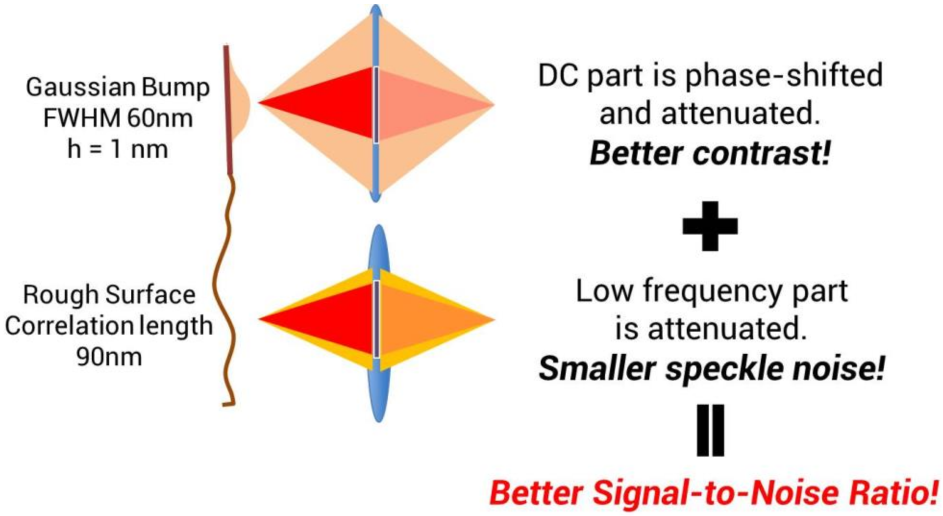

Figure 1.Schematic diagram to show the advantages of the Zernike phase contrast method on EUV mask inspection.

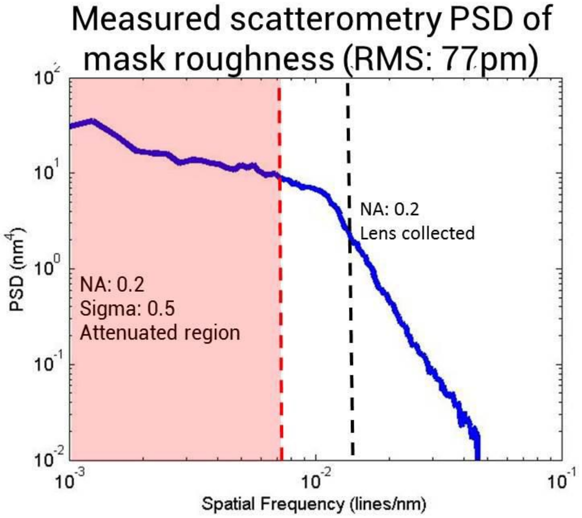

Figure 2. Roughness power spectrum by scatterometry measurement of the EUV mask.

3. SIMULATION RESULTS

3.1 Simulation parameters and settings

Simulation studies using a thin mask scalar imaging model demonstrate the trends in both signal and noise levels. In this study, we consider both phase and amplitude defects with Gaussian and square profiles respectively. For bump defect, the defect height is 1.0 nm and the full width at half maximum (FWHM) ranges from 10 nm to 100 nm. For absorber defect, the width is 10 nm to 100 nm. The width of the line pattern is 44 nm on the EUV mask, which will corresponds to 11 nm at the wafer with the consideration of demagnification in the optical system. The inspection numerical aperture (NA) is 0.2 and the illumination type is disk illumination with a sigma value of 0.5. The phase shift and the apodization in the pupil plane are 0 to 90 degrees and 25% to 100% electric field transmission respectively. Also, the phase shift and apodization region is set to match to the disk illumination at a radius of 0.5 of the pupil in order to control the background light. Table 1 lists the relevant parameters. For mask blank inspection, we define defect signal strength as:

$$\text{Signal Strength} = \left| \frac{Peak\_Intensity - Reference\_Intensity}{Reference\_Intensity} \right| \tag{1}$$

For patterned mask inspection, the defect signal strength definition will be:

$$\text{Signal Strength} = \left| Peak\_Intensity - Reference\_Intensity \right| \tag{2}$$

Table 1. Simulation parameter for the phase contrast method on EUV mask inspection

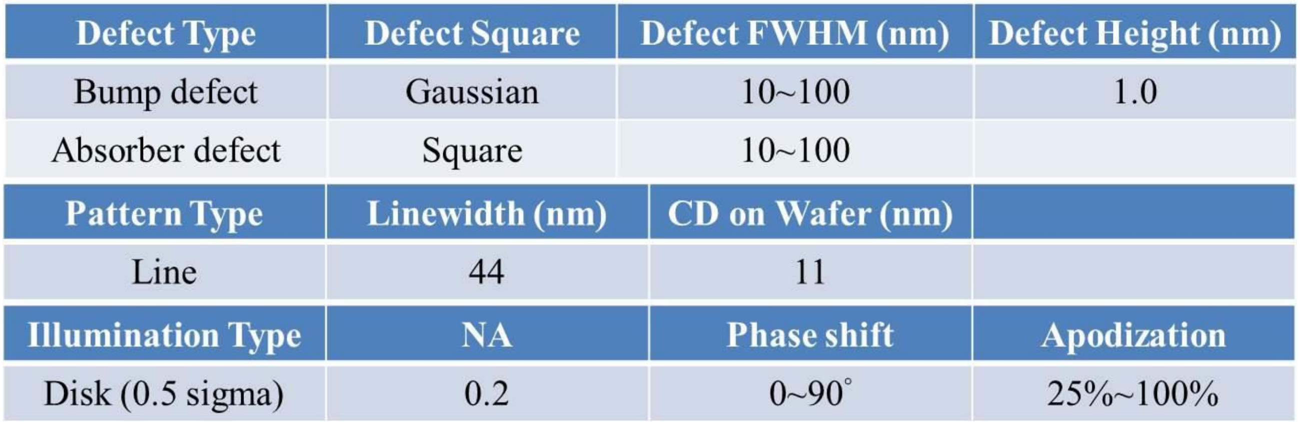

Defect Type	Defect Square	Defect FWHM (nm)	Defect Height (nm)
Bump defect	Gaussian	10~100	1.0
Absorber defect	Square	10~100	
Pattern Type	**Linewidth (nm)**	**CD on Wafer (nm)**	
Line	44	11	
Illumination Type	**NA**	**Phase shift**	**Apodization**
Disk (0.5 sigma)	0.2	0~90°	25%~100%

3.2 Blank inspection: Signal strength

Figure 3(a) shows the signal strength at different defocus positions for a bump defect with and without the Zernike phase contrast method. The height of the defect is 1 nm and the FWHM is 60 nm. As expected, the peak signal strength is at focus for the phase defect when we applied the phase contrast method. However, as shown in Figure 3(b), the position of amplitude defect peak signal strength is moved out of focus when the Zernike phase contrast method is used. Therefore, even with the phase contrast method, we still can only observe one type of defects at focus.

To see if possible to observe both types of defects at focus simultaneously, we simulate the signal strength of phase and amplitude defects at focus with different phase shift from 0 to 90 degrees. The signal strength shown in Figure 4 has been normalized to its maximum value for both types of defects. The height of the phase defect is 1 nm and the FWHM ranges from 20 to 100 nm. The width of the amplitude defects ranges from 20 to 100 nm. As shown in Figure 4, phase defects have maximum signal strength with 90 degree while the amplitude defect signal strength drops to 25% of its maximum value at 90 degrees. By choosing a phase shift about 50 degrees we can achieve an acceptable trade-off between phase and amplitude defect strengths.

With optimized phase shift, one can observe both amplitude and phase defects with a single scan at focus thereby potentially improving inspection throughput.

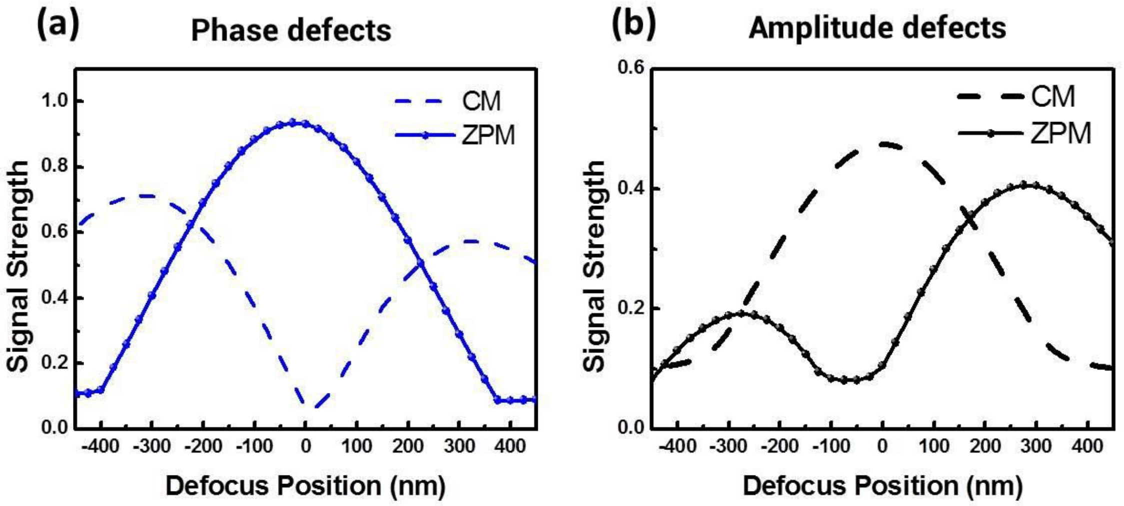

Figure 3. Defect signal strength at different defocus levels with the Zernike phase contrast method (solid curve) and the conventional method (dash curve): (a) Bump defect (Height: 1 nm, FWHM: 60 nm). (b) Amplitude defect (Width: 10 nm).

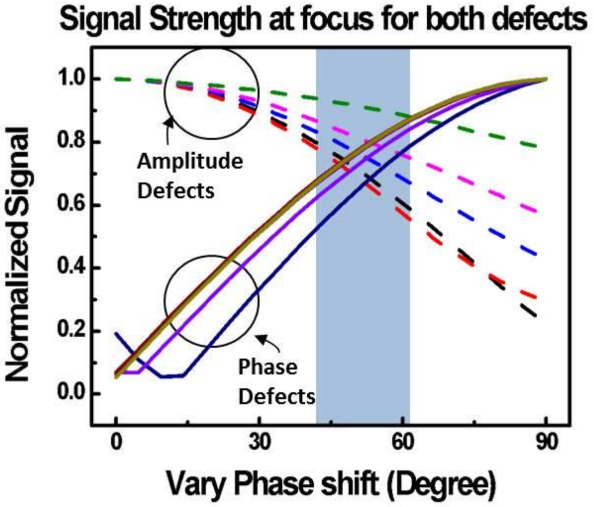

Figure 4. Normalized signal strength at focus for both amplitude and phase defects with different phase shift degree. Shaded area indicates the optimized phase shift region.

3.3 Blank inspection: Signal-to-noise ratio

On EUV masks, multilayer surface roughness plays an important role potentially limiting the inspection SNR. The SNR is defined as the defect signal strength over the speckle noise from surface roughness and the system noise:

$$\mathrm{SNR} = \frac{\mathrm{Defect\_signal}}{\mathrm{Speckle\_noise} + \mathrm{System\_noise}} \tag{2}$$

The system noise can be shot noise, electrical noise, or any other noise sources independent of the mask. With the phase contrast method, both defect signal and phase roughness will be enhanced. Therefore, the improvement of SNR depends on the relationship between speckle and system noise.

Figure 5 shows the SNR at focus for the phase contrast (dark grey) and the conventional methods (light grey) as a function of system noise. The ratio between the two is also shown in blue. The height of the phase defect is 1 nm and the FWHM is 60 nm. The speckle noise is based on the scatterometry data as shown in Figure 2. As shown in Figure 5, the enhancement on SNR by the phase contrast method is larger with larger system noise. The reason is that when the system noise is large relative to the speckle noise, the increase in speckle noise due to the phase contrast method will become negligible. On the other hand, if the speckle noise is larger than the system noise, the increase in speckle noise will offset the increase in signal strength thereby mitigating any improvements in SNR.

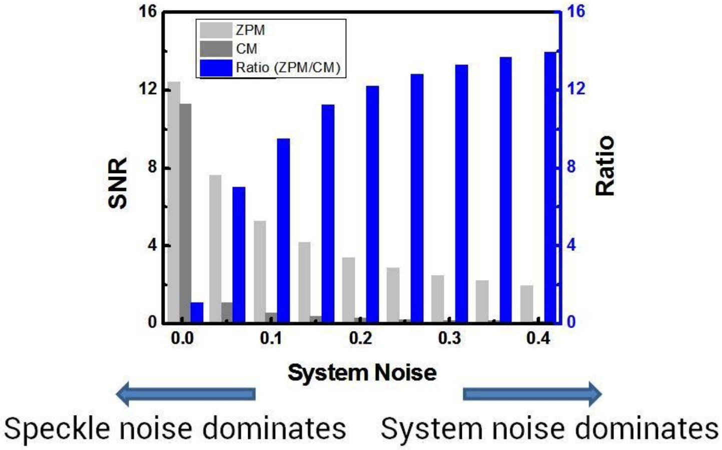

Figure 5. SNR at focus for the phase contrast (dark grey) and the conventional (light grey) methods as a function of system noise. The ratio (blue) of these two values indicates the improvement by the phase contrast method under different system noise.

3.4 Blank Inspection: Optimized phase shift and apodization

In this section, we will consider the optimized phase shift and apodization in terms of SNR at focus for both amplitude and phase defects.

The phase defect is 1 nm in height and the FWHM is 60nm. The width of the absorber defect is 40 nm. The speckle noise is based on the data as shown in Figure 2 and the system noise is set to 5%. We simulate the SNR at focus with 0 degree (conventional), 47 degree (optimized), and 90 degree (phase contrast) in the pupil plane as shown in Table 2. At optimized phase shift, both amplitude and phase defect can achieve a SNR of approximately 7. The difference of SNR between 0 and 47 degree phase shift for amplitude defect comes from the fact that with phase shift in the pupil plane, the amplitude signal strength drops and the speckle noise increase at the same time. We note that selection of the optimal phase shift magnitude and extend in the pupil is expected to be dependent on both the specific shape of defects as well as the PSD of the roughness.

To compensate for the loss in SNR at the optimized phase shift, we can utilize apodization in the pupil plane to increase the contrast of the defect and to also reduce the speckle noise from the surface. To bring the SNR ratios back in balance for these two specific defects at 50% electric field attenuation the Zernike phase shift was lowered to 13 degrees. At this attenuation level the absolute signal intensity is about 75% of the non-attenuated case. The SNR of both types of defects shown in table 2 are approximately 11 when we have 13 degree phase shift in the pupil plane and 50% apodization.

Table 2. SNR of amplitude and phase defects at focus with different phase shift and apodization.

Defect Type	SNR @ focus 0 degree	SNR @ focus 13 degree 50% Apodization	SNR @ focus 47 degree	SNR @ focus 90 degree
Amplitude	18.4	11.1	6.76	2.30
Phase	1.08	11.28	6.6	7.63

3.5 Patterned mask inspection:

To further extend the application of the Zernike phase contrast method, we consider its application to patterned mask inspection in which the pattern in inspected for defects in the blank inspection tool. However, the defects studied will be those deemed to produce CD variations of a maximal critical size when projection printed with dipole illumination. The diffraction from the phase and amplitude defects will be somewhat similar to that in mask inspection. However, given that the NA seen at the mask at 0.2 is 2.4 times larger than 0.0825 used in projection printing, the multiple diffracted orders from the features will introduce considerable complications. Therefore in this initial study, we simply adopted a die-to-database defect detection approach. Here, we identify the effect of defect or roughness by taking die-to-database comparison to extract the variation in the aerial images. Therefore, the ideal background level is zero when we calculate the signal strength. Under this situation, we cannot simply apply apodization to lower the background intensity to get better image contrast as we have for the blank inspection. Figure 6 is the schematic diagram of patterned mask inspection.

As shown in Figure 7, the enhancement of the phase defect peak signal strength depends on its relative position to the absorber pattern. The bump defect is 1 nm in height and the FWHM is 40 nm. The black, blue, and red curves represent the defect beneath the pattern, at the edge, and centered in the space respectively. The improvement in peak signal strength is larger with less pattern overlap. The peak signal strength has 37.8% enhancement compare to the maximum value obtained with the conventional method when the defect is centered at the spacing. For defect is at the edge or beneath the absorber pattern, the enhancement drop to 22.8% and 9.4% respectively. This indicates that the interaction between the phase defect and the absorber pattern will compensate the effect of phase contrast method. However, the maximum signal value remains at focus when there is a 90 degree phase shifts in the pupil plane.

Table 3 shows the SNR for phase and amplitude defects on a patterned mask as a function of different phase shift. These defects are chosen to introduce at least 5% CD variation at the wafer plane by simulation. The maximum SNR for phase and amplitude defects is found at 90 degree and 0 degree Zernike phase shift, respectively. At the optimized phase shift, the SNR for phase defects will be only about 4 and the SNR for amplitude defect can still get 10. The effect of speckle will get worse by a factor of $\sqrt{2}$ if we calculate the effect of roughness based on die-to-die comparison. To further improve the SNR of phase defects for patterned mask inspection, different illumination conditions might be the solution while we cannot use apodization to enhance the contrast and reduce the speckle noise for patterned mask inspection.

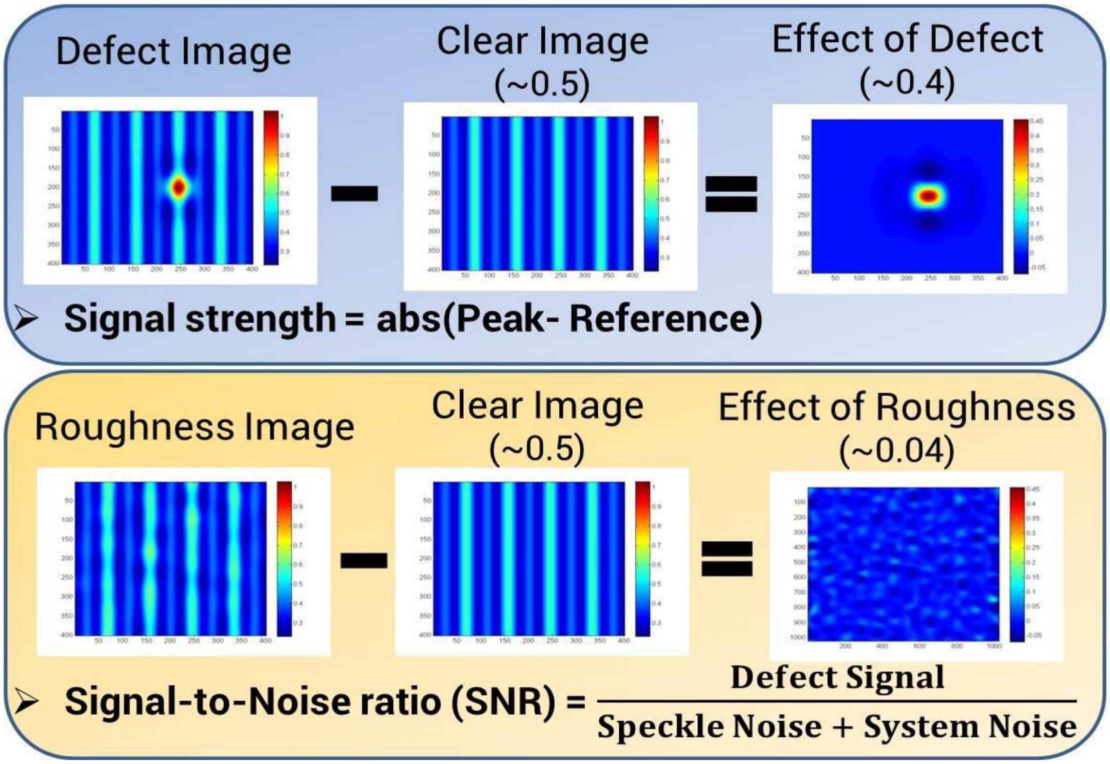

Figure 6. Schematic diagram of patterned mask inspection.

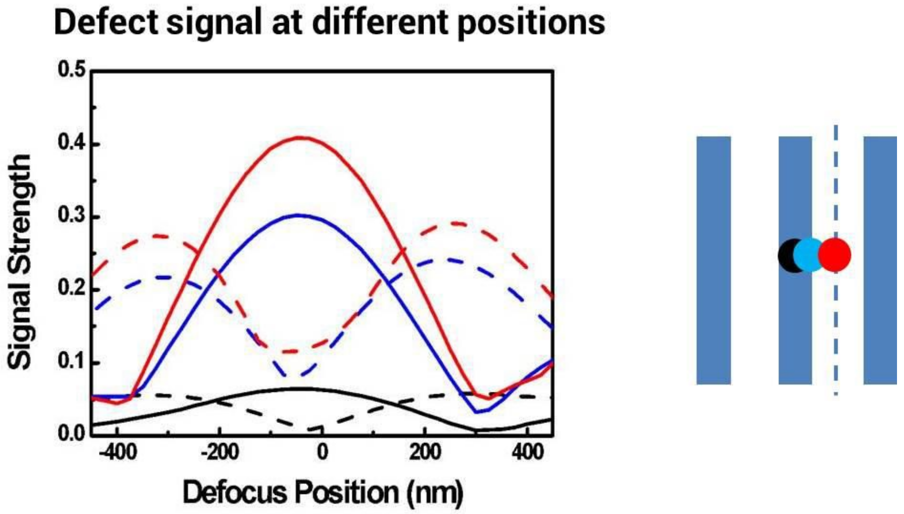

Figure 7. Phase defect (Height: 1 nm, FWHM: 40 nm) signal strength at different defocus levels. Black: beneath the pattern. Blue: at the edge of the pattern. Red: centered at the spacing. Solid curves: phase contrast method. Dash curves: conventional method. The figure on the right shows the relative position of defects on the pattern.

Defect Type	SNR @ focus 0 degree	SNR @ focus 47 degree	SNR @ focus 90 degree
Amplitude at the edge (width: 25nm*50nm)	14.80	***9.63***	4.65
Bump at the spacing (h: 1nm, fwhm: 60nm)	0.92	***3.42***	4.5
Pit at the spacing (h: 1nm, fwhm: 60nm)	0.92	***3.02***	3.58
Bump at the spacing (h: 1.5nm, fwhm: 40nm)	2.48	***3.66***	5.71
Pit at the spacing (h: 1.5nm, fwhm: 40nm)	2.48	***4.74***	4.84

Table 3. SNR of phase and amplitude defects at focus with different phase shifts by patterned mask inspection.

4. CONCLUSION

In this paper, we extend the application of the Zernike phase contrast method to both mask blank and patterned mask inspection. Better defect sensitivity and smaller speckle noise can be achieved with phase shift and apodization in the pupil. For mask blank inspection, optimized phase shift with apodization can further help us observe both amplitude and phase defects at focus simultaneously with an acceptable SNR. This could have significant impact on inspection throughput. For patterned masks, the effectiveness of the phase contrast method depends on the relative positions between phase defects and the absorber pattern.

In future work, we will demonstrate the ideas presented above by implementation of the Zernike phase contrast method in the SEMATECH zoneplate mask inspection microscope (SHARP) at LBNL. Using custom zoneplates, we can control the angular duty cycle to vary the transmission in certain areas (apodization), and also offset the zones in certain areas to create a custom phase shift. Figure 8 shows an SEM image of such zoneplate recently fabricated.

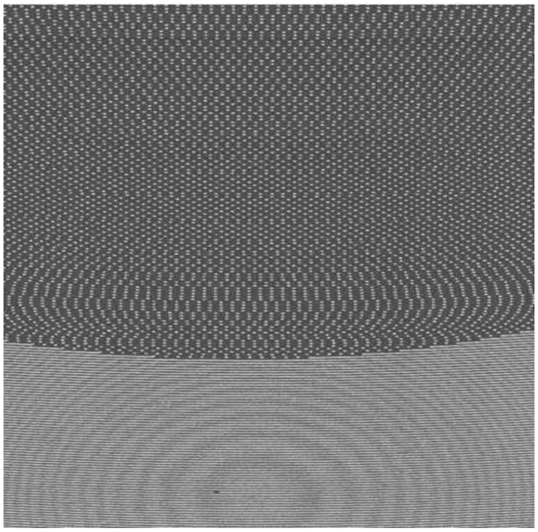

Figure 8. SEM image of an off-axis Fresnel zoneplate with phase shift and apodization.

ACKNOWLEDGEMENT

This research is sponsored by IMPACT+ (Integrated Modeling Process and Computation for Technology). Member companies – Applied Materials, ARM, ASML, Global Foundries, IBM, Intel, KLA-Tencor, Marvell Technology, Mentor Graphics, Panoramic Tech, Photronics, Qualcomm, Samsung, SanDisk and Tokyo Electron.

This work was performed in part at Lawrence Berkeley National Laboratory which is operated under the auspices of the Director, Office of Science, of the U.S. Department of Energy under Contract No. DE-AC02-05CH11231.

REFERENCES

[1] Dan Wack, Yalin Xiong, and Gregg Inderhees, “Solutions for EUV mask and blank inspections,” presented at the 2011 International Symposium on Extreme Ultraviolet Lithography, Miami FL, USA (2011).
[2] Yow-Gwo Wang, Ryan Miyakawa, Andrew Neureuther and Patrick Naulleau, " Zernike phase contrast microscope for EUV mask inspection ", Proc. SPIE9048, 904810 (2014).
[3] Frits Zernike, “How I discover phase contrast,” Science 121, 345-349 (1955).
[4] Rikon Chao, Eric Gullikson, Michael Goldstein, Frank Goodwin, Ranganath Teki, Andy Neureuther and Patrick Naulleau, " EUV scatterometry-based measurement method for the determination of phase roughness ", Proc. SPIE 8880, 88801B (2013).